

Heralded generation of maximal entanglement in any dimension via incoherent coupling to thermal baths

Armin Tavakoli,¹ Géraldine Haack,¹ Marcus Huber,² Nicolas Brunner,¹ and Jonatan Bohr Brask¹

¹*Department of Applied Physics, University of Geneva, 1211 Geneva, Switzerland*

²*Institute for Quantum Optics and Quantum Information (IQOQI),*

Austrian Academy of Sciences, Boltzmannngasse 3, A-1090 Vienna, Austria

(Dated: December 14, 2024)

We present a scheme for dissipatively generating maximal entanglement in a heralded manner. Our setup requires incoherent interactions with two thermal baths at different temperatures, but no source of work or control. A pair of $(d + 1)$ -dimensional quantum systems is first driven to an entangled steady state by the temperature gradient, and maximal entanglement in dimension d can then be heralded via local filters. We discuss experimental prospects considering an implementation in superconducting systems.

I. INTRODUCTION

Entanglement is a key phenomenon distinguishing quantum from classical physics, and is the paradigmatic resource enabling many applications of quantum information science. Generating and maintaining entanglement is therefore a central challenge. Decoherence caused by unavoidable interactions of a system with its environment generally degrades entanglement, and significant effort is invested in minimising the effect of such dissipation in experiments.

However, dissipation can also be advantageous, and may indeed be exploited for the generation of entangled quantum states under the right conditions [1–7]. In particular, it is possible for dissipative processes to drive the system into an entangled steady state [8–11]. This was studied in a variety of physical systems [12–18] and demonstrated experimentally for atomic ensembles [19], trapped ions [20, 21], and superconducting qubits [22]. The main ingredients are engineered decay processes and quantum bath engineering [23–25], and coherent external driving is employed, which, from a thermodynamic point of view, can be considered a source of work.

More generally, it is natural to look for the minimal setting in which dissipative entanglement generation is possible. In particular, one may ask if entanglement can be generated from purely thermal processes alone, without the need for work input or external control. This can in principle be achieved in equilibrium situations, as any entangled state can be obtained as the ground state of a specific Hamiltonian. However, this requires highly nonlocal Hamiltonians which may be extremely difficult to implement in practice.

On the other hand, it was shown that steady-state entanglement can be obtained in systems out of thermal equilibrium. This was first discussed for an atom coupled to two cavities driven by incoherent light [26], and later for many-body systems [27, 28], interacting spins [29, 30], atoms in a thermal environment [31, 32], and mechanical oscillators [33]. In this context, Ref. [34] discussed what is arguably the simplest setting, namely a two-qubit system, where one qubit is connected to a hot

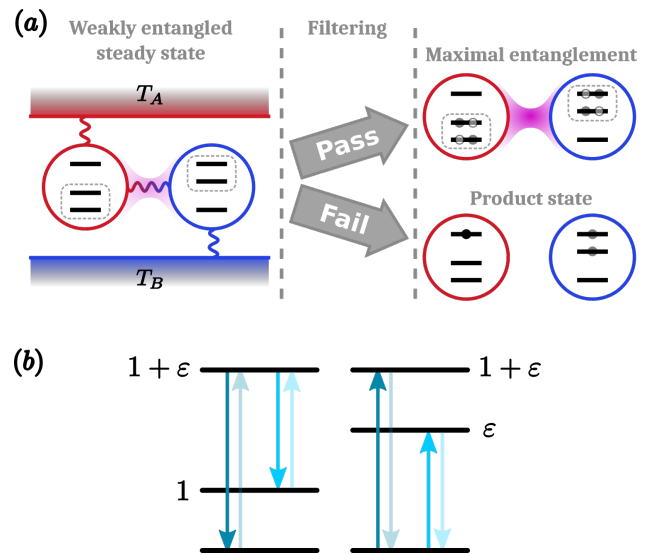


FIG. 1. (a) Qutrit thermal machine. Two qutrits are coupled to each other and to hot and cold thermal baths. The interaction with the baths drives the qutrits into a steady state featuring weak entanglement. Local filters project onto qubit subspaces on each side (dashed boxes). Upon success, the system is projected into a strongly entangled two-qubit state. Failure leaves the qutrits in a separable state, and the process must be restarted. (b) Level structure for the two qutrits. Arrows indicate the transitions involved in the interaction Hamiltonian.

bath and the other to a cold bath. This setup is promising for implementations in superconducting systems and quantum dots. Overall, the out-of-equilibrium approach thus opens interesting perspectives for dissipative entanglement generation. However, its main drawback so far is the fact that the generated entanglement is typically very weak, and thus not directly useful for applications.

Here we offer a solution to this problem, presenting a scheme in which maximal entanglement can be generated in a heralded manner, through incoherent interactions with thermal baths alone. Specifically, a pair of $(d + 1)$ -dimensional systems is first driven to an entangled steady

state, from which maximal entanglement in dimension d can then be heralded via local filters. The procedure is implemented by a simple quantum thermal machine, operating out of equilibrium between two heat baths at different temperatures. Moreover, for $d = 2, 3$ we prove that any pure entangled state can be obtained without additional filtering, indicating that this holds for any d . Finally, we discuss experimental prospects considering an implementation in superconducting systems.

II. TWO-QUTRIT THERMAL MACHINE

The setup we consider is illustrated in Fig. 1(a). Two three-level systems (i.e. qutrits) interact with each other, and independently with two thermal baths at different temperatures T_A and T_B (in the following, $T_A > T_B$ will be the relevant setting for entanglement generation). This out-of-equilibrium situation drives the two-qutrit system into a steady state, which is weakly entangled. A local filter is then applied to each qutrit, projecting the system onto a two-qubit subspace (as indicated by the dashed boxes). If the filter succeeds, the final state is arbitrarily close to a target two-qubit state. This target state can be any pure, entangled state, and in particular may be maximally entangled. If the filter fails, the system is left in a product state with no entanglement, and the process is restarted.

Each qutrit is described by a Hamiltonian H_A , H_B , and their interaction by H_{int} . We take the energy level structure illustrated in Fig. 1(b)

$$H_A = (|1\rangle_A\langle 1| + (1 + \varepsilon)|2\rangle_A\langle 2|) \otimes \mathbf{1}_B, \quad (1)$$

$$H_B = \mathbf{1}_A \otimes (\varepsilon|1\rangle_B\langle 1| + (1 + \varepsilon)|2\rangle_B\langle 2|), \quad (2)$$

where, without loss of generality, we set the ground state energies to zero and the first gap of qutrit A to 1 (throughout the paper, we work in units where $\hbar = k_B = 1$). We are interested in autonomous processes, which require no external work input. This means that H_{int} must be time independent and preserve the total energy, i.e. $[H_{int}, H_A + H_B] = 0$. Writing $|i, j\rangle = |i\rangle_A |j\rangle_B$, we define

$$H_{int} = g_1|0, 2\rangle\langle 2, 0| + g_2|1, 1\rangle\langle 2, 0| + h.c., \quad (3)$$

where g_1 and g_2 denote the interaction strengths. In App. A, we justify this form of H_{int} . For simplicity, we describe the evolution of the system in contact with the thermal baths by a simple reset model [35], leading to the master equation [36]

$$\frac{\partial \rho}{\partial t} = i[\rho, H] + p_A(\tau_A \otimes \text{Tr}_A \rho - \rho) + p_B(\text{Tr}_B \rho \otimes \tau_B - \rho), \quad (4)$$

where $H = H_A + H_B + H_{int}$ is the total Hamiltonian, p_A , p_B are coupling constants, and τ_A , τ_B are thermal states, that is, $\tau_i = \exp(-H_i/T_i)/\text{Tr}[\exp(-H_i/T_i)]$ for $i = A, B$. One can interpret (4) as describing a process

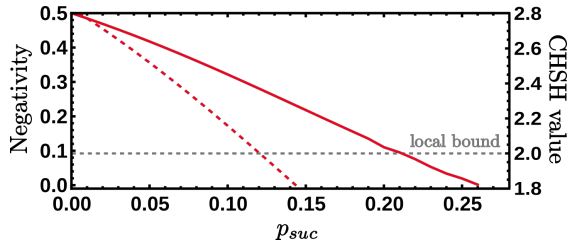


FIG. 2. Optimal negativity (solid, left axis) and CHSH value (dashed, right axis) vs. postselection success probability.

where, at each instance of time, each qutrit is either left unchanged or reset to a thermal state at the temperature of the bath, with resets happening at rates p_A , p_B . To ensure validity of our master equation, we always work in the perturbative regime where $g_1, g_2, p_A, p_B \ll 1, \varepsilon$.

We have derived the steady-state solution $\bar{\rho}$ of (4) in the limit of a maximal temperature gradient, $T_A \rightarrow \infty$, $T_B \rightarrow 0$ (see App. B). To obtain the final state, a local filter is applied to each qutrit, defined by projectors $\Pi_A = |0\rangle_A\langle 0| + |1\rangle_A\langle 1|$ and $\Pi_B = |1\rangle_B\langle 1| + |2\rangle_B\langle 2|$. The normalised, postselected state is

$$\rho' = \frac{1}{p_{suc}}(\Pi_A \otimes \Pi_B)\bar{\rho}(\Pi_A \otimes \Pi_B), \quad (5)$$

where $p_{suc} = \text{Tr}[(\Pi_A \otimes \Pi_B)\bar{\rho}]$ is the probability for the filtering to succeed. We take $g_1 = g \cos(\theta)$ and $g_2 = g \sin(\theta)$. The highest purity for ρ' is obtained when the ratio $\mu = p_A/p_B$ is small. To first order in this ratio, when additionally $g \ll p_B$, one finds the simple expression (restricting to the two-qubit subspace)

$$\rho' = \begin{pmatrix} \frac{1}{3}\mu c_\theta^2 & 0 & 0 & 0 \\ 0 & (1 - \frac{1}{3}\mu)s_\theta^2 & (1 - \frac{2}{3}\mu)c_\theta s_\theta & 0 \\ 0 & (1 - \frac{2}{3}\mu)c_\theta s_\theta & (1 - \frac{1}{3}\mu)c_\theta^2 & 0 \\ 0 & 0 & 0 & \frac{1}{3}\mu s_\theta^2 \end{pmatrix}, \quad (6)$$

where $c_\theta = \cos(\theta)$, $s_\theta = \sin(\theta)$. For $\mu \rightarrow 0$, the state ρ' thus tends to the pure state (relabelling the basis states of the qubit subspace to $|0\rangle, |1\rangle$)

$$|\psi_\theta\rangle = \sin\theta|0, 1\rangle + \cos\theta|1, 0\rangle. \quad (7)$$

Hence, any pure, entangled two-qubit state can be obtained from the qutrit thermal machine (up to local unitaries). In particular, for $\theta = \pi/4$ (i.e. $g_1 = g_2$), we get a maximally entangled state.

We note that although above we took $g \ll p_B$ to get a simple form for (6), this is not crucial. The pure state (7) can be obtained for any value of g , as long as $p_A \ll p_B$ (see App. B). One can understand why higher purity is obtained in this regime since resets induced by the cold bath take the second qubit to the ground state, driving the system out of the postselected two-qubit subspace, while resets induced by the hot bath do not drive the system out of the two-qubit space, but destroys coherence there, reducing the purity.

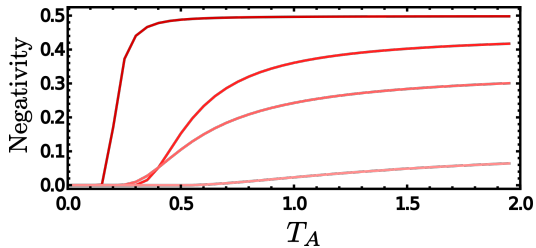


FIG. 3. Entanglement generation for finite temperatures, for varying T_A and (T_B, ϵ) fixed to (from top to bottom) $(0.1, 1.5)$, $(0.2, 1.5)$, $(0.1, 0.5)$, and $(0.2, 0.5)$. To make optimisation over the coupling parameters tractable, we maximise the off-diagonal element of the output state rather than the negativity directly. The curves therefore represent lower bounds.

There is a trade-off between the probability for successful filtering and the quality of ρ' . The success probability tends to zero for both small μ (for fixed g) and small g (for fixed μ). In the two cases, respectively

$$p_{suc} \approx \frac{1}{3} \frac{p_A}{p_B}, \quad \text{and} \quad p_{suc} \approx \frac{2(2p_A + 3p_B)}{9p_B(p_A + p_B)^2} g^2. \quad (8)$$

Adjusting the coupling parameters to increase p_{suc} results in a final state ρ' with a smaller overlap with the target pure state (7). Nevertheless, states of high quality can be generated. In Fig. 2 we show the maximal negativity [37] as well as the value of the Clause-Horne-Shimony-Holt (CHSH) quantity [38] for varying p_{suc} (we optimise over g , p_A , and p_B , while imposing the perturbative regime). We see that ρ' remains entangled up to $p_{suc} \approx 0.25$ and nonlocal up to $p_{suc} \approx 0.12$.

The machine thus provides a heralded source of entangled states: running the machine continuously, the system remains in the steady state until the entangled state is needed, at which point the filtering is performed. If filtering fails, the machine is allowed to return to the steady state, and another attempt can be made. A quasi-deterministic source can be constructed by running several machines in parallel. With n machines, the probability for obtaining a successful projection in at least one of them scales as $1 - (1 - p_{suc})^n$. Failure is exponentially suppressed in n .

In addition to the trade-off between success probability and quality of the postselected state, controlled by the coupling parameters, the temperatures also influence the generated entanglement. So far, we have taken a maximal temperature gradient, $T_A \rightarrow \infty$, $T_B \rightarrow 0$. In Fig. 3 we plot attainable negativity for finite temperatures. We see that, as might be expected, it is always better to take the hot bath temperature as large as possible, maximising the temperature gradient. As the cold bath temperature increases or the gap size ϵ decreases, the hot bath temperature required to generate entanglement increases, and the maximal amount of attainable entanglement decreases. So, to maximise the entanglement, it is desirable to make T_B small and ϵ large (note

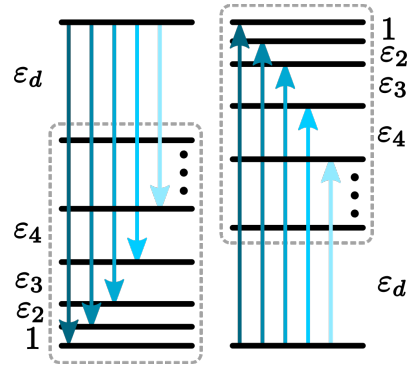


FIG. 4. Level structure of the two $(d + 1)$ -level systems in the qudit thermal machine. Arrows indicate the transitions involved in the interaction Hamiltonian. The dashed boxes indicate the d -dimensional subspaces to which the steady state is filtered to obtain the final state.

though, that p_{suc} decreases with increasing ϵ).

III. TWO-QUDIT THERMAL MACHINE

The scheme considered above can be generalised to create entangled states of two d -level systems, using a $(d + 1)$ -level thermal machine. The setup is the same as in Fig. 1(a), with the qutrits replaced by $(d + 1)$ -level systems, with level structures as illustrated in Fig. 4. Denoting the energy gaps by ϵ_k (with $\epsilon_1 = 1$), and setting $E_k^A = \sum_{l=1}^k \epsilon_l$ and $E_k^B = \sum_{l=1}^k \epsilon_{d-l+1}$, the free Hamiltonians are

$$H_A = \sum_{k=1}^d E_k^A |k\rangle_A \langle k| \otimes \mathbb{1}, \quad H_B = \sum_{k=1}^d \mathbb{1} \otimes E_k^B |k\rangle_B \langle k|, \quad (9)$$

and the interaction Hamiltonian is

$$H_{int} = \sum_{k=1}^d g_k |d, 0\rangle \langle k-1, d-k+1| + h.c., \quad (10)$$

corresponding to the transitions indicated on Fig. 4. The evolution is again described by the master equation (4).

We will focus on the generation of a maximally entangled qudit state

$$|S_d\rangle = \frac{1}{\sqrt{d}} \sum_{k=1}^d |k-1, d-k\rangle. \quad (11)$$

In that case, it suffices to set all the interaction strengths equal, $g_k = g/\sqrt{2}$ (the $\sqrt{2}$ ensures consistency with the qutrit case). In the limit $T_A \rightarrow \infty$, $T_B \rightarrow 0$, the steady state solution of (4) can then be derived analytically for any value of d . It is given in App. C. In analogy with the qutrit case, we consider local projections onto d -dimensional subsystems on each side, given

by $\Pi_A = \mathbb{1} - |d\rangle_A\langle d|$ and $\Pi_B = \mathbb{1} - |0\rangle_B\langle 0|$, and the state after successful filtering is again computed as in (5). We find that, as before, high purity is attained when $p_A \ll p_B$, and the state tends to $|S_d\rangle$, as desired. Thus, our scheme is able to generate maximally entangled states in any dimension. The success probability is given by

$$p_{suc} = \frac{(d-1)g^2 p_A ((d-1)p_A + dp_B)}{d^2 (g^2 \xi + p_A p_B (p_A + p_B)^2)}, \quad (12)$$

where $\xi = (2(d-1)p_A p_B + (d-1)p_B^2 + p_A^2)$. One can check that this agrees with (8) for $d = 3$. Note that p_{suc} scales like $1/d$ for large d , unless $g \sim 1/\sqrt{d}$.

From $|S_d\rangle$, any pure two-qudit state can be obtained via biased filtering and local operations [39]. However, given that any pure, entangled state of two qubits can be generated directly using the qutrit machine by adjusting the coupling strengths, it is natural to ask whether the same holds for qudits. In App. D, we prove this for $d = 3$, suggesting that it generalises to arbitrary d . Note that such direct generation can be advantageous in terms of success probability.

IV. IMPLEMENTATION

A variety of physical platforms might be considered for implementation of our scheme, including trapped atoms, ions, or solid-state artificial atoms. A promising platform is superconducting systems, which are generally good candidates for realizing quantum thermal machines [34, 40–42]. Here, we discuss a potential implementation of the qutrit machine in more detail.

It can be shown that the reset-model master equation above, is equivalent to a Lindbladian master equation plus additional pure dephasing terms (see App. F). The latter can describe the dynamics of two superconducting flux (fluxonium) qutrits [43], weakly interacting and weakly coupled to bosonic baths. More precisely, we consider the setup sketched in Fig. 5(a). The transition frequencies of the fluxonium qutrits are in the range of hundreds of MHz to 30 GHz and are accurately tuneable. An interaction of the form (3) can be implemented in the dispersive regime (resonator frequency far detuned from the qutrit transitions) using two independent resonators. The first term in (3) was already successfully implemented with transmon qubits and is expected to work similarly with fluxonium in the MHz range [44]. There is no fundamental barrier to realising the second term with a second resonator (although some technical difficulties will need to be addressed). A recent numerical work shows that inter-resonator crosstalk should be negligible considering the relevant qutrit (GHz) and interaction (MHz) frequencies [45]. Finally, the coupling rates for the qutrit transitions to the baths are also highly tuneable, from several kHz to a few MHz [43, 44]. The filtering step could be implemented via projective measurements of the highest excited level of qutrit A and

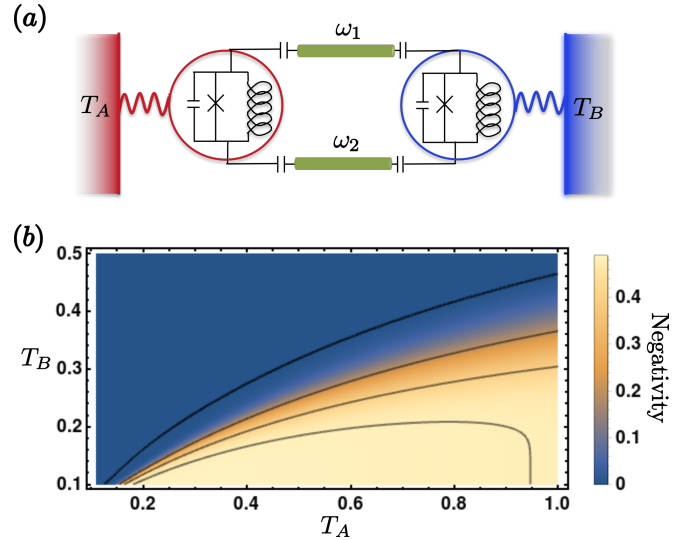


FIG. 5. (a) Implementation of the qutrit machine in circuit QED. Flip-flop type interactions, as in (3), between two fluxonium qutrits are mediated by two microwave resonators with frequencies $\omega_{1,2}$, off resonant with the qutrit energy gaps. (b) Negativity computed from the Lindblad model with parameters $(\Gamma_A, \Gamma_B, \gamma, g, \epsilon) = (10^{-4}, 5 \times 10^{-3}, 3.5 \times 10^{-5}, 1.6 \times 10^{-3}, 3)$. The contours indicate 10^{-5} , 0.2, 0.4, and 0.48.

of the ground state of qutrit B. If occupied, the process fails and no entanglement is generated. If not, the entanglement process is valid. The high tunability of the fluxonium qutrits and their interaction makes them good candidates for implementation.

In Fig. 5(b), we show the negativity computed from the Lindblad master equation description of the fluxonium system, using values for the interaction g , qutrit energies ϵ , bath coupling rates Γ_A, Γ_B , and pure dephasing rate γ which are in agreement with recent experimental achievements in the field [43, 44, 46] (see App. F for details). All parameters are in units of the lowest transition of qutrit A, which is taken to be 1 GHz. The couplings are in the MHz range in order to ensure validity of the Lindblad master equation. We see that strong entanglement can be obtained even including pure dephasing of the qutrits (rate γ in Fig. 5). Negativities above 0.2 can be obtained with success probabilities on the order of 5% as shown in App. F. This implementation would constitute a proof-of-principle demonstration for autonomous, thermal entanglement generation.

V. CONCLUSION

We have demonstrated that combining incoherent couplings to thermal baths out of equilibrium with local filtering enables heralded generation of maximally entangled states in any dimension. The generated states can be made arbitrarily pure, at the price of lowering the

filtering success probability. We have discussed an implementation of our scheme for qubit entanglement in superconducting systems, and found that prospects for a proof-of-principle experiment are good, with significant amounts of entanglement generated in the presence of decoherence and with limited temperature gradients. Interesting future perspectives include thermal generation of multipartite entanglement, and states useful for quantum computation or metrology.

ACKNOWLEDGMENTS

We acknowledge helpful discussions with N. Cottet and B. Huard on implementations in superconducting

systems. We acknowledge the Swiss National Science Foundation (Starting grant DIAQ, grant 200021_169002, and QSIT). GH acknowledges support from the Swiss National Science Foundation through the Marie-Heim Vögtlin grant no. 18874. MH acknowledges funding from the Swiss National Science Foundation (AMBIZIONE PZ00P2_161351) and the Austrian Science Fund (FWF) through the START project Y879-N27.

-
- [1] M. B. Plenio, S. F. Huelga, A. Beige, and P. L. Knight, “Cavity-loss-induced generation of entangled atoms,” *Phys. Rev. A* **59**, 2468–2475 (1999).
- [2] M. S. Kim, Jinhyoung Lee, D. Ahn, and P. L. Knight, “Entanglement induced by a single-mode heat environment,” *Phys. Rev. A* **65**, 040101 (2002).
- [3] L. Jakóbczyk, “Entangling two qubits by dissipation,” *J. Phys. A: Math. Gen.*, 6383 (2002).
- [4] D. Braun, “Creation of entanglement by interaction with a common heat bath,” *Phys. Rev. Lett.* **89**, 277901 (2002).
- [5] F. Benatti, R. Floreanini, and M. Piani, “Environment induced entanglement in markovian dissipative dynamics,” *Phys. Rev. Lett.* **91**, 070402 (2003).
- [6] D. Burgarth and V. Giovannetti, “Mediated homogenization,” *Phys. Rev. A* **76**, 062307 (2007).
- [7] B. Bellomo, R. Lo Franco, S. Maniscalco, and G. Compagno, “Entanglement trapping in structured environments,” *Phys. Rev. A* **78**, 060302 (2008).
- [8] S. Diehl, A. Micheli, A. Kantian, B. Kraus, H. P. Büchler, and P. Zoller, “Quantum states and phases in driven open quantum systems with cold atoms,” *Nat Phys* **4**, 878–883 (2008).
- [9] F. Verstraete, M. M. Wolf, and I. J. Cirac, “Quantum computation and quantum-state engineering driven by dissipation,” *Nat Phys* **5**, 633–636 (2009).
- [10] B. Kraus, H. P. Büchler, S. Diehl, A. Kantian, A. Micheli, and P. Zoller, “Preparation of entangled states by quantum markov processes,” *Phys. Rev. A* **78**, 042307 (2008).
- [11] F. Ticozzi and L. Viola, “Steady-state entanglement by engineered quasi-local markovian dissipation,” *Quant. Inf. and Comp.* **14**, 0265 (2014).
- [12] S. Schneider and G. J. Milburn, “Entanglement in the steady state of a collective-angular-momentum (dicke) model,” *Phys. Rev. A* **65**, 042107 (2002).
- [13] M. J. Kastoryano, F. Reiter, and A. S. Sørensen, “Dissipative preparation of entanglement in optical cavities,” *Phys. Rev. Lett.* **106**, 090502 (2011).
- [14] X. Wang and S. G. Schirmer, “Generating maximal entanglement between non-interacting atoms by collective decay and symmetry breaking,” *arXiv e-print*, 1005.2114 (2010).
- [15] F. Reiter, L. Tornberg, G. Johansson, and A. S. Sørensen, “Steady-state entanglement of two superconducting qubits engineered by dissipation,” *Phys. Rev. A* **88**, 032317 (2013).
- [16] M. J. A. Schuetz, E. M. Kessler, L. M. K. Vandersypen, J. I. Cirac, and G. Giedke, “Steady-state entanglement in the nuclear spin dynamics of a double quantum dot,” *Phys. Rev. Lett.* **111**, 246802 (2013).
- [17] J. Cai, S. Popescu, and H. J. Briegel, “Dynamic entanglement in oscillating molecules and potential biological implications,” *Phys. Rev. E* **82**, 021921 (2010).
- [18] S. Walter, J. C. Budich, J. Eisert, and B. Trauzettel, “Entanglement of nanoelectromechanical oscillators by cooper-pair tunneling,” *Phys. Rev. B* **88**, 035441 (2013).
- [19] H. Krauter, C. A. Muschik, K. Jensen, W. Wasilewski, J. M. Petersen, J. I. Cirac, and E. S. Polzik, “Entanglement generated by dissipation and steady state entanglement of two macroscopic objects,” *Phys. Rev. Lett.* **107**, 080503 (2011).
- [20] J. T. Barreiro, M. Müller, P. Schindler, D. Nigg, T. Monz, M. Chwalla, M. Hennrich, C. F. Roos, P. Zoller, and R. Blatt, “An open-system quantum simulator with trapped ions,” *Nature* **470**, 486–491 (2011).
- [21] Y. Lin, J. P. Gaebler, F. Reiter, T. R. Tan, R. Bowler, A. S. Sørensen, D. Leibfried, and D. J. Wineland, “Dissipative production of a maximally entangled steady state of two quantum bits,” *Nature* **504**, 415–418 (2013).
- [22] S. Shankar, M. Hatridge, Z. Leghtas, K. M. Sliwa, A. Narla, U. Vool, S. M. Girvin, L. Frunzio, M. Mirrahimi, and M. H. Devoret, “Autonomously stabilized entanglement between two superconducting quantum bits,” *Nature* **504**, 419–422 (2013).
- [23] G. Vacanti and A. Beige, “Cooling atoms into entangled states,” *New Journal of Physics* **11**, 083008 (2009).
- [24] F. Reiter, M. J. Kastoryano, and A. S. Sørensen, “Driving two atoms in an optical cavity into an entangled steady state using engineered decay,” *New Journal of Physics* **14**, 053022 (2012).
- [25] C. Aron, M. Kulkarni, and H. E. Türeci, “Steady-state entanglement of spatially separated qubits via quantum bath engineering,” *Phys. Rev. A* **90**, 062305 (2014).
- [26] M. B. Plenio and S. F. Huelga, “Entangled light from white noise,” *Phys. Rev. Lett.* **88**, 197901 (2002).

- [27] L. Hartmann, W. Dür, and H.-J. Briegel, “Steady-state entanglement in open and noisy quantum systems,” *Phys. Rev. A* **74**, 052304 (2006).
- [28] L. Hartmann, W. Dür, and H. J. Briegel, “Entanglement and its dynamics in open, dissipative systems,” *New Journal of Physics* **9**, 230 (2007).
- [29] L. Quiroga, F. J. Rodríguez, M. E. Ramírez, and R. París, “Nonequilibrium thermal entanglement,” *Phys. Rev. A* **75**, 032308 (2007).
- [30] M. Žnidarič, “Entanglement in stationary nonequilibrium states at high energies,” *Phys. Rev. A* **85**, 012324 (2012).
- [31] B. Bellomo and M. Antezza, “Steady entanglement out of thermal equilibrium,” *EPL (Europhysics Letters)* **104**, 10006 (2013).
- [32] B. Bellomo and M. Antezza, “Creation and protection of entanglement in systems out of thermal equilibrium,” *New Journal of Physics* **15**, 113052 (2013).
- [33] D. Boyanovsky and D. Jasnow, “Coherence of mechanical oscillators mediated by coupling to different baths,” *Phys. Rev. A* **96**, 012103 (2017).
- [34] J. B. Brask, G. Haack, N. Brunner, and M. Huber, “Autonomous quantum thermal machine for generating steady-state entanglement,” *New Journal of Physics* **17**, 113029 (2015).
- [35] N. Linden, S. Popescu, and P. Skrzypczyk, “How small can thermal machines be? the smallest possible refrigerator,” *Phys. Rev. Lett.* **105**, 130401 (2010).
- [36] Note that we are using a local master equation, where the dissipation induced by each bath acts locally on the subsystem connected to that bath. Recent works, analysing thermal machines similar to those employed here, have shown such a local approach to provide very good agreement with the exact dynamics for weak coupling, which is the regime of interest here [47, 48].
- [37] G. Vidal and R. F. Werner, “Computable measure of entanglement,” *Phys. Rev. A* **65**, 032314 (2002).
- [38] J. F. Clauser, M. A. Horne, A. Shimony, and R. A. Holt, “Proposed experiment to test local hidden-variable theories,” *Phys. Rev. Lett.* **23**, 880–884 (1969).
- [39] M. A. Nielsen, “Conditions for a class of entanglement transformations,” *Phys. Rev. Lett.* **83**, 436–439 (1999).
- [40] Y.-X. Chen and S.-W. Li, “Quantum refrigerator driven by current noise,” *Europhys. Lett.* **97**, 40003 (2012).
- [41] P. P. Hofer, J.-R. Souquet, and A. A. Clerk, “Quantum heat engine based on photon-assisted cooper pair tunneling,” *Phys. Rev. B* **93**, 041418 (2016).
- [42] P. P. Hofer, M. Perarnau-Llobet, J. B. Brask, R. Silva, M. Huber, and N. Brunner, “Autonomous quantum refrigerator in a circuit qed architecture based on a josephson junction,” *Phys. Rev. B* **94**, 235420 (2016).
- [43] V.E. Manucharyan, *Superinductance*, Ph.D. thesis (2012).
- [44] N. Cottet, “Private communication.”
- [45] Q.-P. Su, H.-H. Zhu, Y. Zhang L. Yu, S.-J. Xiong, J.-M. Liu, and C.-P. Yang, “Generating double noon states of photons in circuit qed,” *Phys. Rev. A* **95**, 022339 (2017).
- [46] A. Kou, W. C. Smith, U. Vool, I. M. Pop, K. M. Sliwa, M. H. Hatridge, L. Frunzio, and M. H. Devoret, “Simultaneous monitoring of fluxonium qubits in a waveguide,” *arXiv e-print*, 1705.05712 (2017).
- [47] P. P. Hofer, M. Perarnau-Llobet, L. D. M. Miranda, G. Haack, R. Silva, J. B. Brask, and N. Brunner, “Markovian master equations for quantum thermal machines: local vs global approach,” *arXiv e-print*, 1705.09211 (2017).
- [48] J. Onam González, L. A. Correa, G. Nocerino, J. P. Palao, D. Alonso, and G. Adesso, “Testing the validity of the local and global GKLS master equations on an exactly solvable model,” *arXiv e-print*, 1705.09228 (2017).
- [49] H.-P. Breuer and F. Petruccione, *The Theory of Open Quantum Systems* (Oxford University Press, Oxford, 2002).
- [50] C. Gardiner and P. Zoller, *Quantum Noise* (Springer-Verlag Berlin Heidelberg, 2004).
- [51] G. Schaller, *Non-Equilibrium Master Equations* (Technische Universität Berlin, 2015).

Appendix A: Choosing the interaction Hamiltonian

Here we explain why the form of the interaction Hamiltonian (3) in the main text is a good choice for entanglement generation. The most general energy conserving interaction involves an additional transition

$$\tilde{H}_{int} = g_1|0,2\rangle\langle 2,0| + g_2|1,1\rangle\langle 2,0| + g_3|1,1\rangle\langle 0,2| + h.c. \quad (\text{A1})$$

However, only the first two transitions contribute to regenerating coherence after thermal resets induced by the baths. When the temperature gradient is maximal ($T_A \rightarrow \infty$, $T_B = 0$), in the reset model, interaction with the baths resets qubit B to its ground state $|0\rangle$, and qubit A to a maximally mixed state. After a reset, the third transition can thus not take place, while the first two transform

$$|2,0\rangle \rightarrow |0,2\rangle \quad \text{with strength } g_1 \quad (\text{A2})$$

$$|2,0\rangle \rightarrow |1,1\rangle \quad \text{with strength } g_2. \quad (\text{A3})$$

As a consequence, the energy levels $|0,2\rangle$ and $|1,1\rangle$ have a non-zero occupation probability. This by itself is not sufficient to generate entanglement, which requires coherent superpositions, but coherence is also induced by the the same interaction because

$$[H_{g_1}, H_{g_2}] = g_1 g_2 (|0,2\rangle\langle 1,1| - |1,1\rangle\langle 0,2|), \quad (\text{A4})$$

where $H_{g_1} = g_1|0,2\rangle\langle 2,0| + h.c.$ and $H_{g_2} = g_2|1,1\rangle\langle 2,0| + h.c.$. The evolution operator defined by H_{int} therefore generates direct transitions between $|0,2\rangle$ and $|1,1\rangle$ and builds coherence between these states. This results in entanglement generation in the subspace spanned by the two-qubit states $\{|0,1\rangle, |0,2\rangle, |1,1\rangle, |1,2\rangle\}$. Note that states $|0,2\rangle$ and $|1,1\rangle$ are degenerate in energy, which is consistent with an energy conserving (autonomous) interaction.

Obviously, the full Hamiltonian (A1) with $g_3 \neq 0$ would also generate entanglement. However, as shown in App. F, this Hamiltonian leads to a decrease of the filtering success probability. Thus, in addition to complicating experimental implementation, the additional term does not help making our heralded generation of maximally entangled states more efficient.

Appendix B: Finding the steady state and filtered state for the two-qutrit machine

Here, we explain how to derive the steady-state solution of the reset model master equation, Eq. (4) of the main text, for two qutrits, and how to obtain the filtered two-qubit state Eq. (6).

The problem of finding an analytical solution is significantly simplified by the following observation: unless the interaction Hamiltonian induces transitions between $|k,j\rangle$ and $|k',j'\rangle$, there can be no coherence between these states in the steady state and the corresponding element in the density matrix vanishes, i.e., $\langle k,j|\rho|k',j'\rangle = 0$. Note that, as seen in the previous section, in addition to the transitions directly present in H_{int} , it also induces second order transitions which need to be taken into account. Following such reasoning, one finds that there are only three non-zero off-diagonal elements in ρ . The density operator then takes the form:

$$\rho = \sum_{k,l=0}^2 q_{kl}|k,l\rangle\langle k,l| + c_0|0,2\rangle\langle 2,0| + c_1|1,1\rangle\langle 2,0| + c_2|0,2\rangle\langle 1,1| + h.c. \quad (\text{B1})$$

where q_{kl} are non-negative numbers that sum to one, and c_0, c_1 and c_2 are complex numbers which we can write as $c_k = v_k + iu_k$ with v_k, u_k real. Plugging this ansatz into the master equation and requiring $\partial\rho/\partial t = 0$, we obtain three independent equations for the off-diagonal terms. Solving the real and imaginary parts of this equation system returns v_k and u_k in terms of the q_{kl} . We are now faced with solving the system of equations corresponding to the diagonal of the right-hand-side of the master equation. This system of eight independent linear inhomogeneous equations can be written in the form $0 = AX + W$ where $X = (q_{00}, q_{01}, \dots, q_{21})^T$ and A is a 8×8 matrix depending on g_1, g_2, p_A and p_B , and W is a 8×1 row-matrix accounting for the inhomogeneous part of the equation system. The solution can then be written $X = -A^{-1}W$. For maximal temperature gradient, $T_A \rightarrow \infty$, $T_B = 0$, this solution can be computed analytically, although the expression is too unwieldy to display here.

Applying the local filters to the steady state, as explained in the main text, and renormalising, one obtains

$$\rho' = \begin{pmatrix} r_1 & 0 & 0 & 0 \\ 0 & r_2 & t & 0 \\ 0 & t^* & r_3 & 0 \\ 0 & 0 & 0 & 1 - r_1 - r_2 - r_3 \end{pmatrix}, \quad (\text{B2})$$

where

$$r_1 = \frac{2p_A \cos^2(\theta) (-g^2 p_A \cos(2\theta) + g^2(p_A + 3p_B) + 3p_B(p_A + p_B)^2)}{(2p_A + 3p_B) (-g^2 p_A \cos(4\theta) + g^2(p_A + 6p_B) + 6p_B(p_A + p_B)^2)} \quad (\text{B3})$$

$$r_2 = \frac{2 \sin^2(\theta) (p_A + 3p_B) (g^2 p_A \cos(2\theta) + g^2(p_A + 3p_B) + 3p_B(p_A + p_B)^2)}{(2p_A + 3p_B) (-g^2 p_A \cos(4\theta) + g^2(p_A + 6p_B) + 6p_B(p_A + p_B)^2)} \quad (\text{B4})$$

$$r_3 = \frac{2 \cos^2(\theta) (p_A + 3p_B) (-g^2 p_A \cos(2\theta) + g^2(p_A + 3p_B) + 3p_B(p_A + p_B)^2)}{(2p_A + 3p_B) (-g^2 p_A \cos(4\theta) + g^2(p_A + 6p_B) + 6p_B(p_A + p_B)^2)} \quad (\text{B5})$$

$$t = \frac{3p_B \sin(2\theta) (g^2(p_A + 3p_B) + 3p_B(p_A + p_B)^2)}{(2p_A + 3p_B) (-g^2 p_A \cos(4\theta) + g^2(p_A + 6p_B) + 6p_B(p_A + p_B)^2)}. \quad (\text{B6})$$

From these expressions, the state Eq. (6) of the main text is recovered in the limit $p_A \ll p_B$ and $g \ll p_B$. The filtering success probability is given by

$$p_{suc} = \frac{2g^2 p_A (2p_A + 3p_B) (g^2 p_A \cos(4\theta) - g^2(p_A + 6p_B) - 6p_B(p_A + p_B)^2)}{9A - 9(B + C + D)}, \quad (\text{B7})$$

where

$$A = g^4 p_A \cos(4\theta) (p_A + p_B) (p_A + 2p_B), \quad (\text{B8})$$

$$B = g^4 (p_A^3 + 11p_A^2 p_B + 26p_A p_B^2 + 12p_B^3), \quad (\text{B9})$$

$$C = 2g^2 p_B (p_A + p_B)^2 (4p_A^2 + 15p_A p_B + 6p_B^2), \quad (\text{B10})$$

$$D = 6p_A p_B^2 (p_A + p_B)^4. \quad (\text{B11})$$

We note that for small p_A or g , the success probability depends only weakly on θ .

Appendix C: Finding the steady state and filtered state for the qudit machine

In the following, we give the steady-state solution of the master equation, Eq. (4) in the main text, for any $d \geq 3$, with the interaction Hamiltonian Eq. (10). We work in the limit $T_A \rightarrow \infty$ and $T_B \rightarrow 0$. That is, we solve

$$0 = i[\rho, H_{int}] + p_A \left(\frac{\mathbb{1}}{d+1} \otimes \text{Tr}_A \rho - \rho \right) + p_B (\text{Tr}_B \rho \otimes |0\rangle\langle 0| - \rho). \quad (\text{C1})$$

Note that we have ignored the free Hamiltonian. We can do that since ρ commutes with the free Hamiltonian in the steady state. This is because H_{int} is energy preserving and can only generate coherence between states of the free Hamiltonians which are degenerate in energy (c.f. the previous section).

We show that the following state solves (C1) for any $d \geq 3$.

$$\begin{aligned} \rho_{d+1} = & \frac{1}{N} \left[\sum_{k,l=0}^d 2g^2 p_A^2 |k,l\rangle\langle k,l| + \sum_{k=0}^{d-1} c_1 |k,0\rangle\langle k,0| + c_2 |d,0\rangle\langle d,0| \right. \\ & + \sum_{k=0}^{d-1} 2(d+1)g^2 p_A p_B |k,d-k\rangle\langle k,d-k| + \sum_{k=0}^{d-1} c_3 |d,0\rangle\langle k,d-k| + h.c \\ & \left. + \sum_{k=1}^{d-1} \sum_{l=1}^{d-k} 2(d+1)g^2 p_A p_B |k+l-1, d-k-l+1\rangle\langle k-1, d-k+1| + h.c \right], \end{aligned} \quad (\text{C2})$$

where we have defined coefficients

$$\begin{aligned} c_1 &= (d+1)p_A p_B (p_A + p_B)^2 + 2g^2 ((d+1)^2 p_B^2 + 2d(d+1)p_A p_B) \\ c_2 &= p_A \left((d+1)p_B (p_A + p_B)^2 + 2(d+1)g^2 d p_B \right) \\ c_3 &= i(d+1)g p_A p_B (p_A + p_B) \\ N &= (d+1)^2 (p_A p_B (p_A + p_B)^2 + 2g^2 (p_A^2 + 2d p_A p_B + d p_B^2)). \end{aligned} \quad (\text{C3})$$

First we compute the following partial traces

$$\text{Tr}_A(\rho) = \frac{1}{N} \left[\sum_{l=0}^d 2(d+1)g^2 p_A^2 |l\rangle\langle l| + (dc_1 + c_2) |0\rangle\langle 0| + \sum_{k=0}^{d-1} 2(d+1)g^2 p_{APB} |d-k\rangle\langle d-k| \right] \quad (\text{C4})$$

$$\text{Tr}_B(\rho) = \frac{1}{N} \left[\sum_{k=0}^d 2(d+1)g^2 p_A^2 |k\rangle\langle k| + \sum_{k=0}^{d-1} c_1 |k\rangle\langle k| + c_2 |d\rangle\langle d| + \sum_{k=0}^{d-1} 2(d+1)g^2 p_{APB} |k\rangle\langle k| \right]. \quad (\text{C5})$$

Subsequently, one can show that

$$\begin{aligned} p_A \left(\frac{\mathbf{1}}{d+1} \otimes \text{Tr}_A \rho - \rho \right) + p_B (\text{Tr}_B \rho \otimes |0\rangle\langle 0| - \rho) = \\ - \frac{1}{N} \left[-2d(d+1)g^2 p_{APB} (p_A + p_B) |d, 0\rangle\langle d, 0| + 2(d+1)g^2 p_{APB} (p_A + p_B) \sum_{k=0}^{d-1} |k, d-k\rangle\langle k, d-k| \right. \\ \left. + c_3 (p_A + p_B) \sum_{k=0}^{d-1} |d, 0\rangle\langle k, d-k| + c_3^* (p_A + p_B) \sum_{k=0}^{d-1} |k, d-k\rangle\langle d, 0| \right. \\ \left. + 2(d+1)g^2 p_{APB} (p_A + p_B) \sum_{k=1}^{d-2} \sum_{l=1}^{d-1-k} (|k+l-1, d-k-l\rangle\langle k-1, d-k| + |k-1, d-k\rangle\langle k+l-1, d-k-l|) \right]. \end{aligned} \quad (\text{C6})$$

Similarly, extensive simplification of the commutator in (C1) gives

$$\begin{aligned} [\rho, H_{int}] = \sum_{k=0}^{d-1} \left(c_2 g - 2d(d+1)g^3 p_{APB} \right) |d, 0\rangle\langle k, d-k| + 2idg \text{Im}(c_3) |d, 0\rangle\langle d, 0| \\ + \sum_{k=0}^{d-1} \left(-c_2 g + 2d(d+1)g^3 p_{APB} \right) |k, d-k\rangle\langle d, 0| - 2ig \text{Im}(c_3) \sum_{k,l=0}^{d-1} |k, d-k\rangle\langle l, d-l|. \end{aligned} \quad (\text{C7})$$

Inserting (C6) and (C7) back into (C1), the verification reduces to two equations

$$i (gc_2 - 2d(d+1)g^3 p_{APB}) = c_3 (p_A + p_B) \quad (\text{C8})$$

$$i (2dgi \text{Im}(c_3)) = -2d(d+1)g^2 p_{APB} (p_A + p_B) \quad (\text{C9})$$

From the definition of c_2 and c_3 , it is easily shown that both these equations are satisfied. Hence, the state (C2) is the steady-state of the thermal machine.

Finally, we show that by applying suitable local filters to ρ , we obtain two maximally entangled d -level systems. The local projectors are

$$\Pi_A = \sum_{k=0}^{d-1} |k\rangle\langle k| \quad \Pi_B = \sum_{l=1}^d |l\rangle\langle l|. \quad (\text{C10})$$

The filtered state becomes

$$\begin{aligned} \rho' = \frac{\Pi_A \otimes \Pi_B \rho \Pi_A \otimes \Pi_B}{\text{Tr}[\Pi_A \otimes \Pi_B \rho]} = \\ \frac{1}{(2g^2 p_A^2 d^2 + 2d(d+1)g^2 p_{APB})} \left[\sum_{k=0}^{d-1} \sum_{l=1}^d 2g^2 p_A^2 |k, l\rangle\langle k, l| + \sum_{k=0}^{d-1} 2(d+1)g^2 p_{APB} |k, d-k\rangle\langle k, d-k| \right. \\ \left. \sum_{k=1}^{d-2} \sum_{l=1}^{d-k-1} 2dgi p_{APB} (|k+l-1, d-k-l\rangle\langle k-1, d-k| + |k-1, d-k\rangle\langle k+l-1, d-k-l|) \right]. \end{aligned} \quad (\text{C11})$$

In the limit $p_A \ll p_B$ this indeed reduces to the maximally entangled state of two d -level systems

$$\rho' = |S_d\rangle\langle S_d| + O\left(\frac{p_A}{p_B}\right). \quad (\text{C12})$$

Appendix D: Generating all pure, entangled states of two qutrits

All pure entangled two-qutrit states can be written using the Schmidt-decomposition as

$$|\psi_{\lambda_1, \lambda_2, \lambda_3}^3\rangle = \sum_{i=0}^2 \lambda_i |i, i\rangle, \quad (\text{D1})$$

with $\lambda \geq 0$ and $\lambda_0^2 + \lambda_1^2 + \lambda_2^2 = 1$. Here, we show that any such state can be generated using a two-ququart thermal machine and local filtering.

The machine consists of two ququarts (four-level systems) with an interaction Hamiltonian

$$H_{int} = g_0(|0, 3\rangle\langle 3, 0| + |3, 0\rangle\langle 0, 3|) + g_1(|1, 2\rangle\langle 3, 0| + |3, 0\rangle\langle 1, 2|) + g_2(|2, 1\rangle\langle 3, 0| + |3, 0\rangle\langle 2, 1|). \quad (\text{D2})$$

Where we choose $g_i = g\lambda_i$ for some small constant g . In the limit of maximal thermal gradient, $T_A \rightarrow \infty$ and $T_B = 0$, the steady-state solution of the master equation can be derived using the method outlined in App. B. The steady state ρ is then filtered to a space of two qutrits corresponding to the projectors $\Pi_A = \mathbb{1} - |3\rangle\langle 3|$ and $\Pi_B = \mathbb{1} - |0\rangle\langle 0|$. The filtered state ρ' depends on $\lambda_0, \lambda_1, \lambda_2, p_A, p_B$ and g . We consider the limit in which $p_A \ll p_B$. This eliminates the dependence on g and p_B . The resulting state is found to be

$$\rho' = |\psi_{\lambda_0, \lambda_1, \lambda_2}^3\rangle\langle \psi_{\lambda_0, \lambda_1, \lambda_2}^3| + O\left(\frac{p_A}{p_B}\right). \quad (\text{D3})$$

Thus, we can generate any pure entangled state of two qutrits.

Based on this result, and the corresponding case for qubits in the main text, we conjecture that any pure entangled state in any dimension can be generated by a generalisation of this thermal machine. Specifically

Conjecture

Let the autonomous thermal machine of two $d + 1$ -level systems coupled to baths of temperature $T_A \rightarrow \infty$ and $T_B = 0$ respectively, operate with an interaction Hamiltonian of the form

$$H_{int} = \sum_{k=0}^{d-1} g_k |d, 0\rangle\langle k, d-k| + h.c. \quad (\text{D4})$$

where we take $g_i = g\lambda_i$ for some small constant g , and where $\{\lambda_i\}_i$ are the Schmidt coefficients of any pure entangled state of two systems of dimension d . Applying the projectors $\Pi_A = \mathbb{1} - |d\rangle\langle d|$ and $\Pi_B = \mathbb{1} - |0\rangle\langle 0|$ to the steady-state of the system, and considering the limit $p_A \ll p_B$, the filtered state becomes

$$|\psi_{\lambda_0, \dots, \lambda_{d-1}}^d\rangle = \sum_{i=0}^{d-1} \lambda_i |i, i\rangle. \quad (\text{D5})$$

In this work, we have shown this conjecture to be true for $d = 2$ and $d = 3$.

Appendix E: Entanglement generation from Hamiltonians with one-step transitions

We consider autonomous thermal machines of two d -level systems with interaction Hamiltonians that only allow energy conserving transitions from one energy-level to a subsequent energy-level, i.e., transitions of the form $|k\rangle \rightarrow |k+1\rangle$ or $|k\rangle \rightarrow |k-1\rangle$. The general form of such a Hamiltonian is

$$H_{int} = \sum_{k=0}^{d-2} g_k (|k+1, d-k-1\rangle\langle k, d-k| + |k, d-k\rangle\langle k+1, d-k-1|), \quad (\text{E1})$$

with $g_k \geq 0$. Again, we work in the limits $T_A \rightarrow \infty$ and $T_B \rightarrow 0$. We seek suitable choices of parameters so that we can generate strong two-qubit entanglement from the filtered steady-state of the thermal machine. To this end, we choose $g_1 = p_B/2$ and $p_A = g_2 = \dots = g_{d-1} \equiv g$. Hence, the only remaining tunable parameters are g and p_B . In order to

obtain a two-qubit system, we project the steady-state ρ_d onto the space spanned by $\{|0\rangle_A, |1\rangle_A, |d-2\rangle_B, |d-1\rangle_B\}$, by applying the projectors $\Pi_A = |0\rangle\langle 0| + |1\rangle\langle 1|$ and $\Pi_B = |d-2\rangle\langle d-2| + |d-1\rangle\langle d-1|$. The filtered state is

$$\rho'_d = \frac{\Pi_A \otimes \Pi_B \rho_d \Pi_A \otimes \Pi_B}{\text{Tr}[\Pi_A \otimes \Pi_B \rho_d]}. \quad (\text{E2})$$

Finally, we apply the limit $g \rightarrow 0$ to the state ρ'_d . For all studied cases, this eliminates the dependence on p_B . We label the resulting state ϱ'_d . We considered $d = 3, \dots, 20$, for all of which we find that ϱ'_d admits the following form

$$\varrho'_d = \begin{pmatrix} 0 & 0 & 0 & 0 \\ 0 & \eta_d & -i\eta_d & 0 \\ 0 & i\eta_d & 1 - \eta_d & 0 \\ 0 & 0 & 0 & 0 \end{pmatrix}, \quad (\text{E3})$$

for some $\eta_d \geq 0$. The negativity of such a state is simply $\mathcal{N} = \eta_d$. For $d = 3, \dots, 8$ we have solved the problem analytically and obtained

$$\eta_3 = \frac{3}{8} = 0.375, \quad (\text{E4})$$

$$\eta_4 = \frac{11}{26} = 0.423, \quad (\text{E5})$$

$$\eta_5 = \frac{89}{199} = 0.447, \quad (\text{E6})$$

$$\eta_6 = \frac{761}{1651} = 0.461, \quad (\text{E7})$$

$$\eta_7 = \frac{26931}{57371} = 0.469, \quad (\text{E8})$$

$$\eta_8 = \frac{243719}{513029} = 0.475. \quad (\text{E9})$$

Furthermore, for $d = 9, \dots, 20$ we have solved the problem numerically using $p_B = 10^{-3}$ and $g = 10^{-12}$, the results are presented in Fig. 6. We observe that the negativity increases with d . For the largest dimension of our consideration,

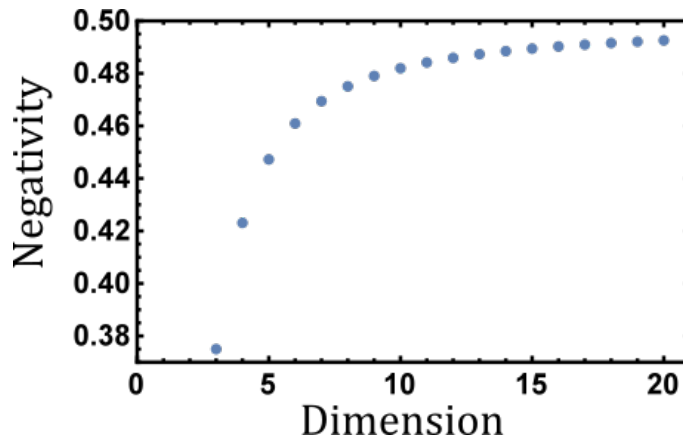


FIG. 6. Lower bounds on the achievable negativity in a thermal machine of two systems, each of dimension d , from which we generate a two-qubit state with one-step transitions.

$d = 20$, we obtained a negativity of 0.4926 and a CHSH value of 2.8075. From these results, we conjecture that the negativity approaches $1/2$ in the limit of large d .

1. Variation of parameters

How much entanglement can be generated if we deviate slightly from the values of the tunable parameters given above? We consider this issue for the simplest cases, namely $d = 3, 4$. In particular, we relax the requirement

$g_1 = p_B/2$ and instead write it as $g_1 = gp_B$ for some $0 \leq g$. Calculating the steady-state solution of the master equation, performing the above stated projections onto a qubit-qubit subspace, taking the limit $g \rightarrow 0$, and calculating the negativity of the resulting state, we obtain

$$\mathcal{N}(d=3) = \frac{3-g}{2+8g} \quad \mathcal{N}(d=4) = \frac{g(5+2g^2)}{3+13g^2+4g^4} \quad (\text{E10})$$

We see that for any positive g , the state is entangled. In Figure 7 we plot these two negativities.

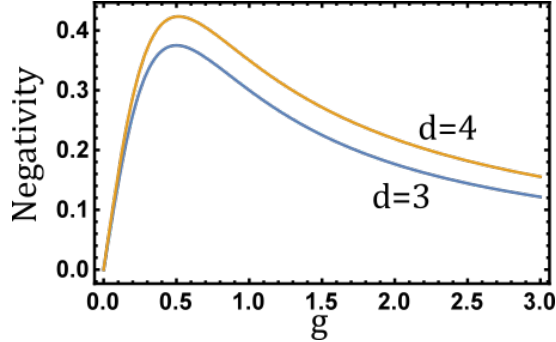


FIG. 7. Plots of negativity as functions of g for $d=3$ and $d=4$.

Appendix F: Implementation

1. Lindbladian master equation

The reset model considered in the main text is intuitive, amenable to analytical analysis, and captures the essential physics of a multipartite quantum system in contact with thermal baths. However, instantaneous thermal resets are a simplification with respect to realistic implementations.

More realistic master equation can be obtained from microscopic models of the baths and the system-bath interaction. The dynamics of quantum systems weakly coupled to thermal baths has been extensively investigated in previous works [49–51]. In the regime where all the interactions and couplings strengths are small compared to the typical energy gaps of the system, the dynamics is well captured by a master equation in the Lindblad form. For bosonic baths (which corresponds to our implementation proposal), the Lindblad master equation takes the form

$$\dot{\rho}(t) = -i[H, \rho(t)] + \sum_i \Gamma_i n_B(E_i, T_i) \mathcal{D}[A_i^+] \rho(t) + \sum_i \Gamma_i (1 + n_B(E_i, T_i)) \mathcal{D}[A_i^-] \rho(t), \quad (\text{F1})$$

where H and ρ are the Hamiltonian and state of the system. The superoperator \mathcal{D} is defined as $\mathcal{D}[A_i] \rho = A_i \rho A_i^\dagger - 1/2\{A_i^\dagger A_i, \rho\}$, and A_i^\pm are jump operators. These account for dissipation processes due to excitation exchange between the system and the bath at coupling strength Γ_i . Excitations flow from the baths to the system with rates $\Gamma_i^+ \equiv \Gamma_i n_B(E_i, T_i)$ and from the system to the baths with rates $\Gamma_i^- \equiv \Gamma_i (1 + n_B(E_i, T_i))$. Here $n_B(E_i, T_i) = 1/(e^{E_i/T_i} - 1)$ is the Bose-Einstein distribution at energy E_i and temperature T_i .

An equation of the type (F1) is appropriate for describing a realistic implementation of our thermal machine, for instance using Fluxonium qutrits coupled to a bosonic environment (see also [34]). In the following, we focus on the two-qutrit machine. The Hamiltonian can be taken as in the main text (and as before, because the interaction is energy conserving, only H_{int} gives a nontrivial contribution to the commutator).

2. Correspondence between reset model and Lindbladian master equation

Here, we see that the conditions to get maximally entangled states derived for the reset model, $T_A \rightarrow \infty$, $T_B \rightarrow 0$, $p_A \ll p_B$ do not translate directly to the Lindblad model. However, as explained in the main text and below, it is still possible to generate entanglement arbitrarily close to maximal.

To proceed, we first evaluate the dynamics of the populations and derive under which conditions they match for the two models. We start with the most general form of (F1), *i.e.* by including the couplings and corresponding jump operators between all energetic transitions $|0\rangle_i - |1\rangle_i, |0\rangle_i - |2\rangle_i, |1\rangle_i - |2\rangle_i$ for qutrit $i=A,B$ and their respective thermal bath set by temperature T_A, T_B . The identification term by term for the 9 populations give us the following conditions for qutrit A

$$\Gamma_i^+ n_B(E_i, T_A) = \Gamma_i^- (1 + n_B(E_i, T_A)) = \frac{p_A}{3} \quad \text{for all transitions } i = 01, 02, 12, \quad (\text{F2})$$

and for qutrit B

$$\Gamma_{01}^- (1 + n_B(E_{01}, T_B)) = \Gamma_{02}^- (1 + n_B(E_{02}, T_B)) = p_B, \quad (\text{F3})$$

$$\Gamma_{12}^- (1 + n_B(E_{12}, T_B)) = \Gamma_i^+ n_B(E_i, T_B) = 0. \quad (\text{F4})$$

We immediately notice that these equalities can not be satisfied when taking into account form of the Bose-Einstein distribution n_B . Therefore, the limits and optimal regime found within the reset model can not be achieved when considering a state-of-the-art experiment. In a realistic setup, one can not demand that excitations only flows in one direction, the coupling rates must satisfy the Gibbs ratio,

$$\frac{\Gamma_i^+}{\Gamma_i^-} = e^{-E_i/T_i} \quad (\text{F5})$$

3. Experimental proposal

To model a potential implementation of our scheme using fluxonium qutrits, we use a master equation of the type (F1) augmented by additional dephasing of the excited levels of each qutrit. The negativity shown in Fig. 5 of the main text is obtained from the following model

$$\begin{aligned} \dot{\rho}(t) = & -i[H_{int}, \rho(t)] + \sum_{k=A,B} \left(\sum_{i=01,02,12} \Gamma_{ik} n_B(E_i, T_k) \mathcal{D}[A_i^+] \rho(t) + \sum_{i=01,02,12} \Gamma_{ik} (1 + n_B(E_i, T_k)) \mathcal{D}[A_i^-] \rho(t) \right) \\ & + \gamma (\mathcal{D}[\sigma_z^{A1} \otimes \mathbb{1}] + \mathcal{D}[\sigma_z^{A2} \otimes \mathbb{1}] + \mathcal{D}[\mathbb{1} \otimes \sigma_z^{B1}] + \mathcal{D}[\mathbb{1} \otimes \sigma_z^{B2}]) \rho(t) \end{aligned} \quad (\text{F6})$$

Following Ref. [46], we take the pure dephasing rate equal to $5 \cdot 10^{-4}$ GHz. The coupling rates to the thermal baths are assumed to be the same for the three transitions ($\Gamma_{ik} \equiv \Gamma_k, k = A, B$), but different for the two qutrits

$$\Gamma_A = 10^{-4} \text{ GHz}, \quad (\text{F7})$$

$$\Gamma_B = 5 \cdot 10^{-3} \text{ GHz}. \quad (\text{F8})$$

We also provide the form of the different jump operators. We use a local master equation description, where each jump operator A_j^\pm is of the form $\sigma_i^\pm \otimes \mathbb{1}_3$ or $\mathbb{1}_3 \otimes \sigma_i^\pm$, *i.e.* it acts only on qubit A or qubit B. This is well justified as long as the inter-qutrit interaction is not much stronger than the coupling to the baths [47, 48]. The thermal jump operators are defined by

$$\sigma_{01}^+ = \begin{pmatrix} 0 & 0 & 0 \\ 1 & 0 & 0 \\ 0 & 0 & 0 \end{pmatrix}, \quad \sigma_{01}^- = \begin{pmatrix} 0 & 1 & 0 \\ 0 & 0 & 0 \\ 0 & 0 & 0 \end{pmatrix}, \quad (\text{F9})$$

$$\sigma_{02}^+ = \begin{pmatrix} 0 & 0 & 0 \\ 0 & 0 & 0 \\ 1 & 0 & 0 \end{pmatrix}, \quad \sigma_{02}^- = \begin{pmatrix} 0 & 0 & 1 \\ 0 & 0 & 0 \\ 0 & 0 & 0 \end{pmatrix}, \quad (\text{F10})$$

$$\sigma_{12}^+ = \begin{pmatrix} 0 & 0 & 0 \\ 0 & 0 & 0 \\ 0 & 1 & 0 \end{pmatrix}, \quad \sigma_{12}^- = \begin{pmatrix} 0 & 0 & 0 \\ 0 & 0 & 1 \\ 0 & 0 & 0 \end{pmatrix}. \quad (\text{F11})$$

The pure dephasing operators only affect the coherences of the density operator (there is no relaxation process associated to it). We only consider such dephasing for the two excited levels of each qutrits $|1\rangle, |2\rangle$. The operators are

$$\sigma_z^{i1} = \begin{pmatrix} 0 & 0 & 0 \\ 0 & 1 & 0 \\ 0 & 0 & 0 \end{pmatrix}, \quad \sigma_z^{i2} = \begin{pmatrix} 0 & 0 & 0 \\ 0 & 0 & 0 \\ 0 & 0 & 1 \end{pmatrix}. \quad (\text{F12})$$

with $i = A, B$.

The results for the negativity and success probability are shown in Fig. 8. For completeness, we show them by considering on one side the optimal interaction Hamiltonian (3) as argued in App. A and on the other side the most general one given by (A1). Interestingly, the more general form provides neither better negativity nor higher success probability, even at non-maximal temperature gradient. On the contrary, the success probability (red curve) is lower, while the negativity is the same for the two cases (blue curve). This shows that (3) is not only simpler one to implement but also optimizes the success probability for generating entangled states.

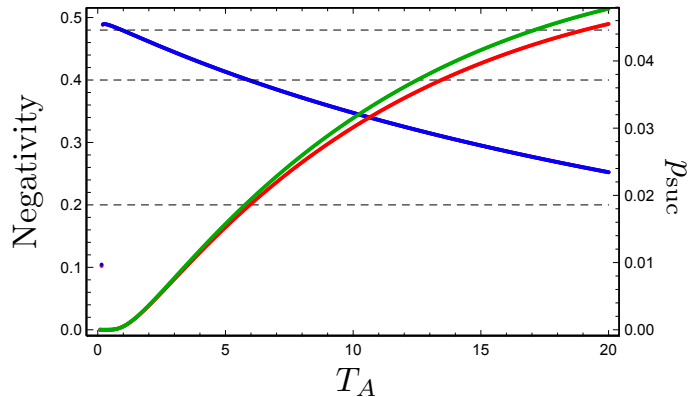


FIG. 8. Negativity and success probability as a function of temperature T_A .

Fig. 8 also confirm what was derived analytically: the implementation of the thermal machine is not compatible with the optimal conditions found for the reset model, see above (F2) and (F3). The negativity (blue curve) is maximal for a small temperature gradient, which is imposed by the bosonic statistics of the bath excitations. The corresponding success probability is very small ($< 0.1\%$). However, a negativity between 0.2 and 0.4 can be achieved with a success probability 3 and 5% (green and red curves). This makes this scheme a reasonable proposal to demonstrate heralded entanglement using incoherent couplings to thermal baths.

Appendix G: Some other autonomous thermal machines for entanglement generation

In this section, we briefly present results for entanglement generation obtained from autonomous thermal machines consisting of either two qubits, or a qubit and a qutrit.

1. Qubit-qubit machine

An autonomous qubit-qubit machine for entanglement generation was previously considered in [34]. Without loss of generality we set the energy spectrum of each qubit to be $(0, 1)$. The interaction Hamiltonian is $H_{int} = g(|0, 1\rangle\langle 1, 0| + |1, 0\rangle\langle 0, 1|)$. We have solved the steady-state master equation for $T_A \rightarrow \infty$ and $T_B \rightarrow 0$. The steady-state reads

$$\rho_{qubits} = \frac{1}{2s^2(2g^2 + p_A p_B)} \begin{pmatrix} p_A p_B s^2 + g^2 t^2 & 0 & 0 & 0 \\ 0 & g^2 p_A t & -i g p_A p_B s & 0 \\ 0 & i g p_A p_B s & p_A (p_B s^2 + g^2 t) & 0 \\ 0 & 0 & 0 & g^2 p_A^2 \end{pmatrix}, \quad (\text{G1})$$

where $s = (p_A + p_B)$ and $t = (p_A + 2p_B)$.

Numerically optimizing the negativity of this state returns

$$\mathcal{N} = 0.004 \text{ obtained with: } g \approx 2.2 \times 10^{-3} \quad p_A \approx 2.3 \times 10^{-3} \quad p_B \approx 9.5 \times 10^{-3}. \quad (\text{G2})$$

We note that in the previous work considering this machine [34], the entanglement measure was chosen as the concurrence. The state which achieves the above negativity is not the state achieving the optimal concurrence found in [34]. The optimal state thus depends on the entanglement measure of choice.

2. Qubit-qubit machine with population inversion

We now extend the above considered qubit-qubit machine with the possibility of population inversion, i.e., we imagine that there is another thermal machine coupled to (the hot) qubit A that allows us to invert the population of the thermal state so that it becomes $\tau_A = |1\rangle\langle 1|$. This corresponds to a Boltzmann distribution in which $T_A \rightarrow 0^-$ and $T_B \rightarrow 0$. Allowing for such a possibility, the steady-state solution of the master equation becomes,

$$\rho_{\text{qubits}} = \frac{1}{(p_A + p_B)^2 (2g^2 + p_A p_B)} \begin{pmatrix} 2g^2 p_B^2 & 0 & 0 & 0 \\ 0 & 2g^2 p_A p_B & -ig p_A p_B (p_A + p_B) & 0 \\ 0 & ig p_A p_B (p_A + p_B) & p_A p_B (2g^2 + (p_A + p_B)^2) & 0 \\ 0 & 0 & 0 & 2g^2 p_A^2 \end{pmatrix}. \quad (\text{G3})$$

For simplicity we put $p_A = p_B$, and calculate the negativity to be zero if $g \geq p_B$, whereas if $g < p_B$ we obtain

$$\mathcal{N} = \frac{g(p_B - g)}{2(2g^2 + p_B^2)}. \quad (\text{G4})$$

The largest negativity is found for $g = \frac{p_B}{1+\sqrt{3}}$. The resulting state has purity 0.758 and a negativity $\mathcal{N} = \frac{\sqrt{3}-1}{8} \approx 0.092$. This constitutes a significant improvement over the qubit-qubit machine without population inversion [34]. The obtained negativity coincides with what was obtained by numerical optimization of the negativity of (G3).

3. Qubit-qutrit machine

Here we consider an autonomous thermal machine consisting of one qubit (system A) and one qutrit (system B). The energy spectrum of the qubit is $(0, 1)$ whereas the energy spectrum of the qutrit is chosen as $(0, 1, 2)$. There are two resonant transitions. The interaction Hamiltonian reads

$$H_{\text{int}} = g_1 (|0, 1\rangle\langle 1, 0| + |1, 0\rangle\langle 0, 1|) + g_2 (|0, 2\rangle\langle 1, 1| + |1, 1\rangle\langle 0, 2|). \quad (\text{G5})$$

Take the qubit to be cold ($T_A \rightarrow 0$), and the qutrit to be hot ($T_B \rightarrow \infty$). We have solved the steady-state master equation in terms of g_1, g_2, p_A and p_B . As we are interested in two-qubit entanglement, we project the qutrit onto the space spanned by its two upper energy-levels. For the resulting two-qubit state ρ' we consider the limit in which $p_B \rightarrow 0$. That returns the state

$$\rho' = \frac{1}{2g_2^2 p_A^2 + g_1^2 (8g_2^2 + p_A^2)} \begin{pmatrix} 2g_2^2 (2g_1^2 + p_A^2) & 0 & 0 & 0 \\ 0 & g_1^2 (2g_2^2 + p_A^2) & ig_1^2 g_2 p_A & 0 \\ 0 & -ig_1^2 g_2 p_A & 2g_1^2 g_2^2 & 0 \\ 0 & 0 & 0 & 0 \end{pmatrix}. \quad (\text{G6})$$

We can optimise the magnitude of the off-diagonal terms by picking $p_A = \frac{2\sqrt{2}g_1 g_2}{\sqrt{g_1^2 + 2g_2^2}}$. Subsequently, we take $g_2 \rightarrow 0$ which causes all instances of g_1 to cancel out. The resulting state, which has a purity of $17/32$ and negativity $\mathcal{N} = \frac{\sqrt{3}-1}{8} \approx 0.092$, which is the same as obtained above with a two-qubit machine with population inversion. However, the entangled state obtain here is significantly more mixed than what was obtained with two qubits and population inversion. Nevertheless, a larger negativity can be obtained for our current thermal machine: performing a numerical optimization of the negativity of (G6) we find

$$\mathcal{N} = 0.104, \text{ obtained for: } g_1 \approx 9.2 \times 10^{-3} \quad g_2 \approx 4.8 \times 10^{-7} \quad p_A \approx 2.1 \times 10^{-6}. \quad (\text{G7})$$

The corresponding state has purity 0.6875.

4. Qubit-qutrit machine with population inversion

For the qubit-qutrit machine, we now allow for the possibility of population inversion of the qubit through the use of another thermal machine coupling to it. This corresponds to $T_A \rightarrow 0^-$ and $T_B \rightarrow 0$. The two-qubit subspace is obtained from the steady-state by projecting onto the lower two energy-levels of the qutrit. For the resulting state ρ' , we take $p_B \rightarrow 0$ and obtain

$$\rho' = \frac{1}{g_2^2 p_A^2 + g_1^2 (6g_2^2 + p_A^2)} \begin{pmatrix} 0 & 0 & 0 & 0 \\ 0 & 2g_1^2 g_2^2 & -ig_1 g_2^2 p_A & 0 \\ 0 & ig_1 g_2^2 p_A & g_2^2 (2g_1^2 + p_A^2) & 0 \\ 0 & 0 & 0 & g_1^2 (2g_2^2 + p_A^2) \end{pmatrix}. \quad (\text{G8})$$

The negativity of this state is

$$\mathcal{N} = \frac{-g_1^2 (2g_2^2 + p_A^2) + \sqrt{4g_1^2 g_2^4 p_A^2 + g_1^4 (2g_2^2 + p_A^2)^2}}{2(g_2^2 p_A^2 + g_1^2 (6g_2^2 + p_A^2))}. \quad (\text{G9})$$

To find a large value of this expression, we put $p_A = Kg_1$ for some positive constant K . Then, we let $g_1 \rightarrow 0$. We find

$$\mathcal{N} = \frac{-g_2^2 + \sqrt{g_2^4 (1 + K^2)}}{g_2^2 (6 + K^2)}. \quad (\text{G10})$$

To find the optimal value of K , we solve $\partial\mathcal{N}/\partial K = 0$. There are two positive solutions, of which we pick $K = \sqrt{6 + 2\sqrt{6}}$, which returns

$$\mathcal{N} = \frac{1}{2 + 2\sqrt{6}} \approx 0.145. \quad (\text{G11})$$

This value coincides with the numerical maximization of the negativity of the state (G8).